

Spin dynamics in hole-doped NiO from ^7Li NMR in $\text{Ni}_{1-x}\text{Li}_x\text{O}$

M. Corti, S. Marini,* A. Rigamonti, and F. Tedoldi

Department of Physics 'A. Volta,' Unita' INFN and Sezione INFN, Via Bassi 6, I-27100 Pavia, Italy

D. Capsoni and V. Massarotti

Department of Physical Chemistry, University of Pavia, I-27100 Pavia, Italy

(Received 28 January 1997; revised manuscript received 2 June 1997)

^7Li NMR spectra and relaxation measurements in $\text{Ni}_{1-x}\text{Li}_x\text{O}$ ($0.01 \leq x \leq 0.2$) are presented for external fields ranging from 1 T up to 9.4 T in the temperature range $10 \leq T \leq 700$ K. Insights into the effect of the doping on the correlated spin dynamics of the $S=1$ Ni^{2+} in the paramagnetic (PM) and in the antiferromagnetic (AF) phases are achieved. In the PM phases the ^7Li relaxation rates W are related to the critical dynamics of the Ni^{2+} spins. It is found that the slowing down of the spin fluctuations is characterized by critical exponents having little x dependence, while the Néel temperature decreases with x approximately in the form $T_N(x) = T_N(0)[1 - 2.2x]$, faster than theoretical predictions for cubic Heisenberg systems or for dilution by localized diamagnetic impurities. In the AF phase the hopping of the holes induces fluctuating fields at the nuclear site which are responsible for a sizable contribution to the ^7Li W . One derives the gaps between itinerant and localized-charge transfer states. These gaps turn out to be larger than in CuO and decreasing on increasing x , in substantial agreement with electrical conductivity. At a temperature $T_m(x)$, which decreases with increasing x , the hopping frequencies reach the radio-frequency range and the holes localize on the oxygen nearest neighbors to the Li^+ impurities. Then another relaxation mechanism arises, inducing marked maxima in W at a x -independent temperature $T^* \approx 130$ K, with a recovery described by a stretched exponential. This low-temperature relaxation mechanism is attributed to progressive freezing of the spin fluctuations of effective magnetic moments generated by the hole localization which interact through the AF matrix and correspond to a disordered paramagnet. The activation energy for the freezing is found $E_A \approx 1300$ K, supported also by muon depolarization-rate measurements. [S0163-1829(97)00341-X]

I. INTRODUCTION

NiO is a prototype of the $3d$ -transition-metal oxides (TMO's), with a strong d - d correlation which yields an insulating character.¹ The charge fluctuations are suppressed since the correlation gap is much larger than the one-electron dispersive bandwidth.² Thus the low-energy magnetic properties involve the $3d^8$ $S=1$ Ni^{2+} ions. The superexchange interaction through O^{2-} leads to an antiferromagnetic (AF) state, with Néel temperature $T_N = 524.5$ K.³ Hole doping of TMO's plays a key role in high- T_c superconducting materials and a deep understanding of the electrical and magnetic properties of the nonstoichiometric compounds is considered a step necessary for dealing with the mechanism underlying superconductivity in cuprates.⁴ NiO can be doped by substituting Li^+ for Ni^{2+} . $\text{Ni}_{1-x}\text{Li}_x\text{O}$, up to $x \approx 0.25$, keeps its fcc crystalline structure and the low-temperature AF ordered state, with T_N decreasing with increasing x . The holes compensating the Li^+ impurity charge are of $\text{O}(2p)$ character, with a strong AF exchange interaction with localized Ni^{2+} $S=1$ d electrons.⁴ On the basis of general aspects of t - J models and by extending the findings to other TMO's, the holes can iterate on the AF matrix, although the impurity potential due to Li^+ tends to bind them in localized states.² The resistivity is expected to be of the form⁵ $\rho \propto (T/\nu_0 x) \exp[E_h/T]$, where ν_0 is the Debye frequency, while the activation energy E_h of the spin-dependent hopping mechanism is related to the magnetic exchange^{6,7}

Of great interest in doped TMO's are the magnetic prop-

erties and the related spin dynamics. The properties of NiO are well described by localized magnetic moments with a Heisenberg-like spin-only Hamiltonian, the orbital momenta being practically quenched by crystal or ligand fields much larger than the spin-orbit terms. Hole doping on $S=1$ Heisenberg systems has recently triggered a great deal of attention. An effective low-energy Hamiltonian, suitable to describe the role of mobile holes and analogous to the one introduced by Zhang and Rice to reduce the two-dimensional multiband Hubbard model to the t - J model,⁸ has recently been proposed by Dagotto *et al.*⁹ From the solution of this Hamiltonian for a small cluster, the hole-hopping process and related Ni^{2+} spin dynamics can be described as follows. The O-type hole forms a singlet with one Ni hole, leaving an $S=1/2$ low-energy state at a given site. This state can easily switch to an adjacent site, producing an effective hopping process which corresponds to a transition from the $S=1/2$ to $S=1$ state of the Ni ion. This process, in turn, corresponds to fluctuations of the Ni^{2+} spin operators around the Li^+ ions and the ^7Li NMR relaxation can detect this spin dynamics.

The ^7Li spin-lattice relaxation rate, in fact, is given by

$$1/T_1 = \frac{\gamma^2}{2} \int \langle h_+(0)h_-(t) \rangle e^{-i\omega_L t} dt, \quad (1)$$

where γ is the nuclear gyromagnetic ratio and $\omega_L = \gamma H_0$, while h_{\pm} are the transverse components (with respect to $\vec{H}_0 \parallel \vec{z}$) of the effective fictitious field $\vec{h}(t)$ at the Li site.

Here $\vec{h}(t)$ is given by

$$\vec{h} = \sum_J \vec{A}_J \cdot \vec{S}_J - g\mu_B \sum_J \frac{1}{r_J^3} \left[\vec{S}_J - \frac{3\vec{r}_J(\vec{r}_J \cdot \vec{S}_J)}{r_J^2} \right], \quad (2)$$

where A_J describes the hyperfine interaction while the second term represents the dipolar interaction with the J th Ni ion. The temperature and doping dependence of the AF static field at the Li site, due to the sublattice local magnetization $\langle S_J \rangle$, is obtained from the Li NMR spectra. At low temperatures, where the holes become localized, further spin excitations, related to the freezing of the effective magnetic moments, are also detected by ${}^7\text{Li}$ NMR relaxation.

A study of this type has been already carried out through ${}^7\text{Li}$ NMR relaxation in Li-doped CuO.¹⁰ Relevant effects due to itinerant holes in generating Cu^{2+} spin fluctuations have been evidenced from the marked maxima in T_1^{-1} at a temperature T^* which is a function of the amount of doping and of the measuring frequency ν_L . For light Li concentration ($x \approx 0.01$) some evidence of hole localization was also found.¹¹ The basic ${}^7\text{Li}$ NMR relaxation mechanisms in $\text{Ni}_{1-x}\text{Li}_x\text{O}$ are analogous to the ones in $\text{Cu}_{1-x}\text{Li}_x\text{O}$. However, in the present case of Li-doped NiO the process related to the progressive freezing of the mobile holes and the one due to the slowing down of the fluctuations of the magnetic moments associated with the localization are clearly evidenced through two maxima in T_1^{-1} occurring in different temperature ranges.

Finally, in the paramagnetic phase of NiO we have studied the critical dynamics driving the transition to the ordered state and the effect of doping on the spin fluctuations is investigated.

The paper is organized as follows. In Sec. II, after some details of experimental character and on the methodology of the measurements, the experimental results for the spectra and for the relaxation rates are presented, establishing the proper relationships of the NMR quantities to the static and dynamical magnetic properties. Section III is devoted to a thorough analysis of the results in terms of the role of doping on the critical dynamics [paramagnetic (PM) phase], of the hole-hopping process in the high-temperature AF phase (phase AF I), and in the temperature range (phase AF II) where the holes are localized. Finally, in Sec. IV, summarizing remarks and conclusions are reported.

II. EXPERIMENTAL AND RESULTS

A. Samples and NMR general aspects

The $\text{Ni}_{1-x}\text{Li}_x\text{O}$ compounds have been prepared¹² by the reactive system $\text{NiO}/\text{Li}_2\text{CO}_3$ heated up to 800°C and annealed in alumina, with a cooling rate of 5°C min^{-1} . The sample composition and structure have been controlled by x-ray-diffraction measurements, with a Philips PW 1710 powder diffractometer. As already noticed,¹³ Li^+ was found to substitute Ni^{2+} in an equivalent lattice position and, for $x \leq 0.25$ the NiO cell (pseudocubic at room temperature) with NaCl structure type ($Fm\bar{3}m$), is still preserved. The lattice parameter of the pseudocubic cell, as a function of the Li content, is reported in Fig. 1.

The occurrence of the transition to an AF phase and the Néel temperatures $T_N(x)$ have been detected from the ${}^7\text{Li}$ NMR spectra and from the peaks in the relaxation rate (see

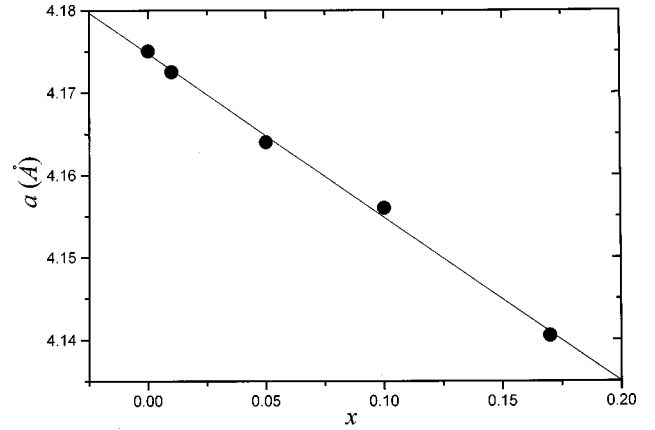


FIG. 1. Lattice parameter of the pseudocubic cell of $\text{Ni}_{1-x}\text{Li}_x\text{O}$ as a function of the Li content. The solid line is the best-fit behavior according to a linear decrease of a with increasing x .

later on). The transition temperature was found to be independent of the external field H_0 , within the experimental errors, up to $H_0 \approx 5.9$ T, for $x = 0.1$.

The ${}^7\text{Li}$ NMR measurements have been carried out by means of Bruker spectrometers (MSL 200 and AM 400) with a high-power unit allowing a radio-frequency (rf) field H_1 of amplitude up to 100 G, in external fields $H_0 = 5.9$ T and $H_0 = 9.4$ T. At lower fields, namely, H_0 from 0.7 T to 2 T, homemade spectrometer designed for long-term stabilization and acquisition was used. The temperature range of measurements was 10–700 K, with thermal stability better than 1° .

${}^7\text{Li}$ NMR spectra in the PM phase, for narrow lines, have been obtained by Fourier transforming (FT) half of the echo signal following the quadrupolar echo pulse sequence $(\pi/2)_x - \tau - (a\pi/2)_y - \pi/2$ corresponding to the pulse length maximizing the signal in a solution of LiCl. For broad lines the spectra have been reconstructed from the envelope of the FT of the echo signals collected at different irradiation frequencies. A small quadrupole interaction on the ${}^7\text{Li}$ nucleus was observed, likely due to a slight distortion of the cubic structure around the impurity. In view of the small value of the quadrupole coupling constant the spread of the ${}^7\text{Li}$ NMR frequency due to the angular-dependent electric perturbation is smaller than the rf spectral distribution and in practice both the central ($1/2 \leftrightarrow -1/2$) and the two satellite ($\pm 3/2 \leftrightarrow \pm 1/2$) lines are irradiated. The signal, in fact, was maximized by a pulse length equal to the one in the LiCl solution, where the static quadrupole interaction is averaged to zero. For $a = 2$ the quadrupolar echo sequence is expected to generate an echo from the central line, while for $a = 1$ the satellites transitions, broadened by a first-order quadrupole interaction, are also refocused in the echo.

In the AF phase the Li NMR spectra show a large broadening due to the field $\langle h_z \rangle$ of dipolar origin [second term in Eq. (2)] and a slight shift resulting from the hyperfine term. For a linewidth of the order of the rf distribution the NMR lines have been still reconstructed by FT the echo signals collected at different frequencies. For very broad lines, the spectra have been obtained by the echo envelope as a function of the irradiation frequency, by reducing the strength of the rf field.

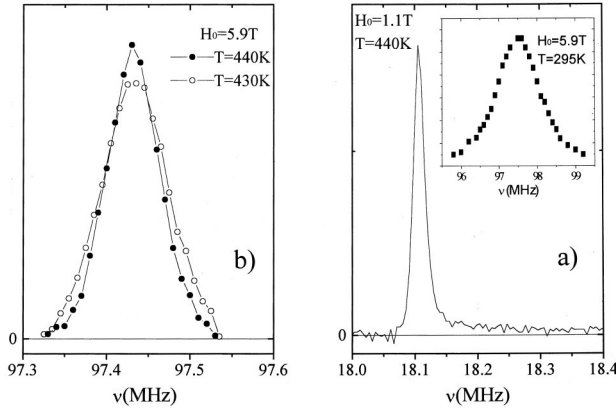


FIG. 2. ${}^7\text{Li}$ NMR spectra in the paramagnetic phase of $\text{Ni}_{0.9}\text{Li}_{0.1}\text{O}$. The line at $H_0 = 1.1$ T (a) has been obtained by FT half of the echo signal, while the spectra at $H_0 = 5.9$ T (b) have been reconstructed from the envelope of the FT of the echo as collected at different irradiation frequencies. The temperature and field dependence of the linewidth indicates a broadening of the form $\delta\nu = a + bH_0$, with $a \approx 11$ kHz while $b \approx 9.3$ kHz/T is the dipolar contribution due to $\langle \mu_{\text{Ni}} \rangle_H = \chi_a H_0$ (see text). On approaching T_N the broadening is consistent with the increase of χ_a . The inset of part (a) shows an illustrative example of the spectra in the AF phase.

The spin-lattice relaxation times have been obtained from the recovery of the echo signal after a sequence of saturating pulses at the central frequency of the correspondent spectrum. Both central and satellite lines were thus irradiated and in general the recovery of the ${}^7\text{Li}$ echo signal is well described by an exponential law, with no dependence on the length of the saturating sequence. The time constant of the recovery is therefore $T_1 = (2W)^{-1}$, W being the relaxation transition probability due to the time-dependent part of the field given by Eq. (2). For very broad lines the small, fast-recovering part of the echo signal, related to the spectral diffusion, was not considered and only a part (about 90%) of the exponential form was taken into account to extract T_1 . Around the peak in the relaxation rate observed in the phase AF II (see later on), the recovery was no longer described by an exponential law. The relevance of this changeover will be discussed (Sec. III) in term of spin-glass-like behavior upon localization of the holes.

B. ${}^7\text{Li}$ NMR spectra

In the paramagnetic phase the ${}^7\text{Li}$ NMR frequency was found to be close to the one of the reference signal in the LiCl solution, indicating that the scalar part of the nucleus-electron interaction [first term in Eq. (2)] is small. The dipolar part [second term in Eq. (2)], when averaged over the random orientation in a polycrystalline sample, yields a broadening of the line. Through $\langle h_z \rangle \propto \langle S_z \rangle = \chi_a H_0$ this broadening tracks the atomic susceptibility χ_a of the Ni^{2+} ion. An order of magnitude estimate for the broadening expected from the first 12 Ni^{2+} ion nearest neighbors to a given Li nucleus, by using the experimental value^{3,14} of the susceptibility, yields $\delta\nu \approx (10 \text{ kHz}) H_0$ (H_0 in tesla), in agreement with the experimental results (see Fig. 2).

Below T_N the spontaneous sublattice magnetization induces a nonzero local field \vec{h}_{AF} at the Li site. While h_{AF}

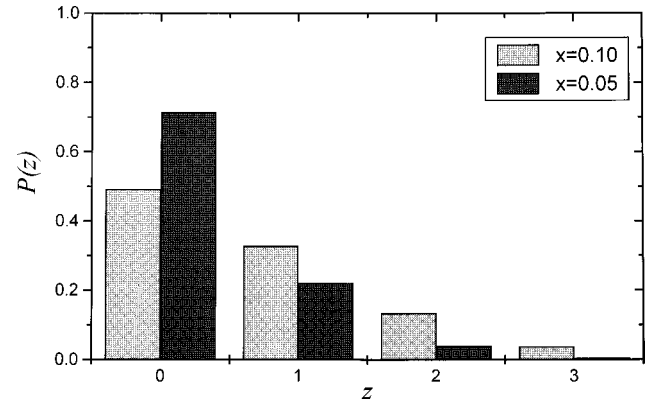


FIG. 3. Probability for a given Li^+ reference ion to have z other Li^+ ions as nearest neighbors, in $\text{Ni}_{1-x}\text{Li}_x\text{O}$, for $x = 0.1$ and $x = 0.05$.

would be zero in the case of a perfect cubic arrangement of AF ordered magnetic moments, the non-magnetic Li^+ ions break the AF symmetry and one has $\vec{h}_{\text{AF}} \neq 0$. Thus a marked, temperature-dependent, broadening of the line is observed. The shift of the line is difficult to evidence, again consistent with a largely dipolar origin of the \vec{h}_{AF} field. For instance at $T \approx 350$ K, in $\text{Ni}_{0.9}\text{Li}_{0.1}\text{O}$ the shift is within 0.01% for $H_0 \approx 1$ T, with a linewidth of the order of 700 G.

The shape of the line in the AF phase is related to the powder distribution of \vec{h}_{AF} with respect to \vec{H}_0 . From the relation $p(\nu) \propto [dh_z/d(\cos\theta)]^{-1}$, with $h_z = |\vec{h}_{\text{AF}}| \cos\theta$ one would expect a rectangular shape of the line, of width $\Delta\nu = 2\gamma/(2\pi)|\vec{h}_{\text{AF}}|$. In $\text{Ni}_{1-x}\text{Li}_x\text{O}$ one has to take into account the fields experimented by Li nuclei having different numbers of other Li^+ ions at the nearest-neighbors (NN) Ni sites. The probability for a given Li ion to have other Li's as nearest neighbors (and thus $h_{\text{AF}} \neq 0$) can be evaluated as follows. The probability of having z Li^+ in a cluster of 13 sites is $P'_{13,x}(z) = 13! x^z (1-x)^{13-z} / z!(13-z)!$. Then one has to renormalize in order to reduce the estimate only to those cases in which one ion (the reference one) is at least present: $P_x(z) = P'_{13,x}(z+1) / [1 - P'_{13,x}(0)]$. The results are plotted in Fig. 3 for the samples at $x = 0.05$ and $x = 0.1$. As a consequence, one has a distribution of rectangular shape which cause a NMR line consistent with the one shown in the inset of Fig. 2. Being mostly interested in the temperature dependence of the sublattice magnetization to which \vec{h}_{AF} is proportional, we will simply use the full width at half intensity ΔH of the ${}^7\text{Li}$ spectra as a measure of the local field. In Fig. 4 the temperature dependences of ΔH , for $x = 0.05$ and $x = 0.1$, are shown.

C. ${}^7\text{Li}$ relaxation rates

The ${}^7\text{Li}$ relaxation rates are reported in Fig. 5. In the inset of the figure $1/T_1$ around the transition is reported in detail, showing how from the maxima the Néel temperatures $T_N(x)$ were estimated. These temperatures coincide within the experimental errors with the ones where the onset of \vec{h}_{AF} at the Li site was indicated by a marked broadening of the spectra. The recovery of the ${}^7\text{Li}$ echo signal after complete saturation in general was described by an exponential law. Around

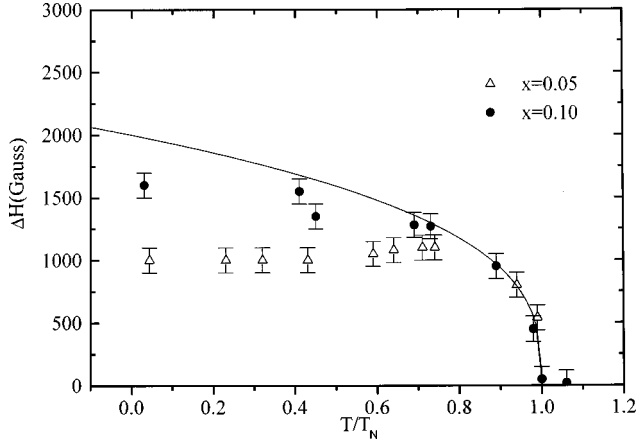


FIG. 4. Temperature dependence of the local field $|\vec{h}_{\text{AF}}(x, T)|$, as obtained from the width ΔH of the ^7Li NMR spectra for $x=0.05$ (\triangle) and $x=0.1$ (\bullet). The solid line represents the best-fit behavior of the data for $T/T_N \geq 0.7$ according to the law $|\vec{h}_{\text{AF}}| \propto \Delta H \propto (T_N - T)^{1/3}$.

$T \approx 130$ K, where the relaxation rates have marked maxima, the recovery is no longer exponential and the data reported in Fig. 5 are the inverse of the time at which the recovery plot reduces to $1/e$.

For high temperatures, namely, $T \geq 750$ K, the relaxation rates have been noticed to increase on increasing temperature

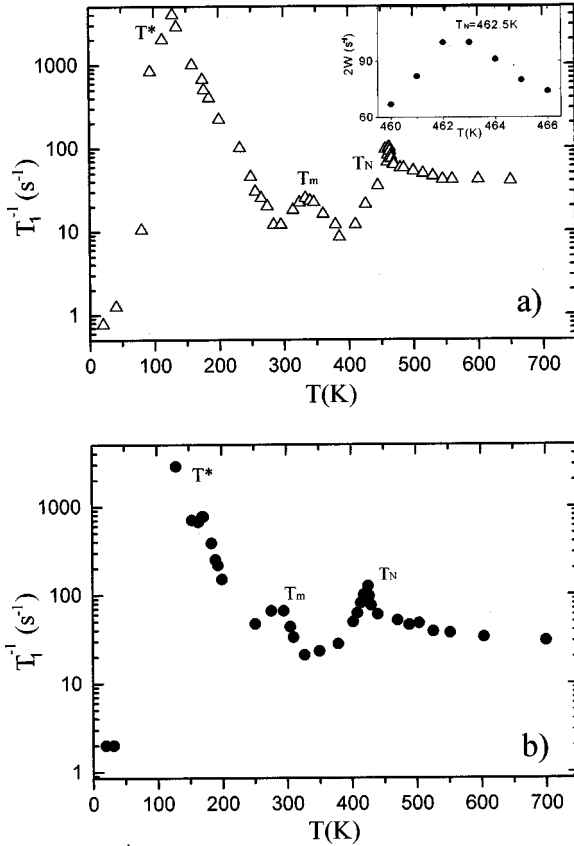


FIG. 5. ^7Li NMR spin lattice relaxation rate $1/T_1 = 2W$ as a function of temperature in $\text{Ni}_{1-x}\text{Li}_x\text{O}$ for $x=0.05$ (a) and $x=0.1$ (b). The inset is a blowup of the results around the transition from the paramagnetic to the antiferromagnetic phase and indicates how $T_N(x)$ was evaluated (see text).

(data not reported in Fig. 5), probably related to diffusion of Li^+ ions which induces a further relaxation mechanism. In the slow-motion condition (diffusion frequency $\nu_d \ll \nu_L^2$), this contribution can be written $T_1^{-1} \propto \nu_d / \nu_L^2$, implying a relaxation rate which increases with increasing rate of diffusion. The diffusion of Li^+ ions has no effect at lower temperature, the relaxation process being controlled by the spin fluctuations driving the time dependence in the field $\vec{h}(t)$ at the Li site, as is proved by the maxima in T_1^{-1} at the transition from the PM to the AF phase.

III. ANALYSIS OF THE DATA AND DISCUSSION

In this section the results pertaining to the static quantities, such as fields at the Li site, and the ^7Li relaxation rates due to the time dependence of the dipolar field are discussed. It is convenient to consider three different temperature ranges: the PM phase ($T > T_N$); the AF phase I, where the holes itinerate, which spans approximately from T_m to T_N , T_m being the temperature at which the relaxation rates show maxima (Fig. 5); a second AF phase (AF II) will be considered, approximately below 250 K, where the holes are localized and cause a strong contribution to the relaxation rates around $T^* \approx 130$ K.

A. Paramagnetic phase

For $T \geq T_N$ the extra hole is moving very fast and does not appreciably contribute to the nuclear relaxation process. The ^7Li NMR relaxation is controlled by the relatively slow dynamics of Ni^{2+} $S=1$ spins. In the limiting situation of infinite temperature, with uncorrelated spin fluctuations, the relaxation rate can be expressed in the form¹⁵

$$\frac{1}{T_1} = \frac{2}{3} \gamma^2 g^2 \mu_B^2 S(S+1) \sum_J \frac{1}{r_J^6} \tau_e, \quad (3)$$

with

$$\tau_e = \frac{\sqrt{2\pi}}{\omega_e} = \sqrt{2\pi} \frac{\sqrt{3}\hbar}{[2J_{1e}^2 K_B^2 z S(S+1)]^{1/2}}, \quad (4)$$

where z is the number of NN spins and J_{1e} is the effective exchange interaction between NN. The exchange constants of the undoped system can be taken as $J_1 = |-34|$ K for the nearest neighbors and $J_2 = 202$ K for the next-nearest neighbors.³ For an order of magnitude estimate one can limit the summation in Eq. (3) to the NN lattice sites, at the distance $r_{\text{NN}} = 2.96$ Å, where $n(x) = 12\{1 - [1 - P_x(0)]/12\}$ magnetic ions are placed with $J_{1e} \approx J_1(1-x)^2$. Then

$$\frac{1}{T_1} \approx \frac{4}{3} \gamma^2 g^2 \mu_B^2 n(x) \frac{1}{r_{\text{NN}}^6} \frac{\sqrt{6\pi}\hbar}{2\sqrt{12}J_{1e}K_B}. \quad (5)$$

From Eqs. (4) and (5), for $x=0.1$ one derives $T_1^{-1} \approx 150$ s⁻¹, larger than the experimental data by a factor of about 6. This discrepancy is consistent with the occurrence of a correlated spin dynamics. The AF correlation leads to a sizable reduction of the relaxation rate since the filtering effect implies a cancellation of the effective field at the critical wave vector. For a single Ni^{2+} ion missing in the cluster of the 12 NN of

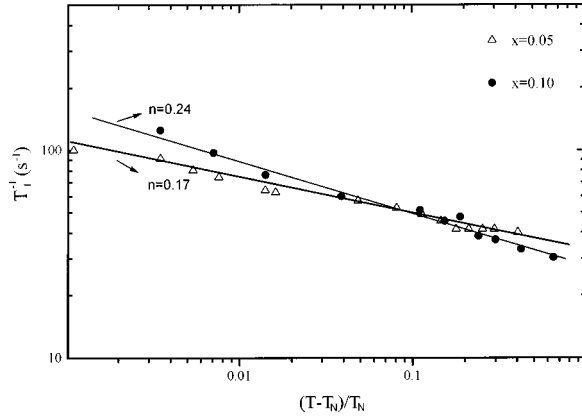


FIG. 6. Log-log plot of the ${}^7\text{Li}$ NMR relaxation rate in the PM phase of $\text{Ni}_{1-x}\text{Li}_x\text{O}$ as a function of the reduced temperature $(T-T_N)/T_N$.

a given Li^+ (the condition pertaining to about 40% of the nuclei; see Fig. 3) one obtains an order of magnitude of T_1 close to the experimental data. Let us discuss the temperature dependence of the ${}^7\text{Li}$ T_1 in the PM phase by referring for simplicity to the case of an effective fluctuating field associated with a spin vacancy NN of a given Li nucleus. By introducing collective spin components $S_q^-(t)$ and decay rates Γ_q^- of the normal excitations, one can write¹⁵

$$\frac{1}{T_1} = \frac{2}{3} \gamma^2 g^2 \mu_B^2 \frac{1}{r_{\text{NN}}^6} \frac{1}{N} \sum_q \frac{\langle |S_q^-|^2 \rangle}{\Gamma_q^-} \quad (6)$$

and then relate the relaxation rate to the exchange Heisenberg frequency ω_e through the magnetic correlation length ξ ,¹⁶

$$\frac{1}{T_1} = \gamma^2 g^2 \mu_B^2 \frac{1}{r_{\text{NN}}^6} \frac{1}{\omega_e} \left(\frac{\xi}{a} \right)^{z-d+2-\eta} \quad (7)$$

z is the dynamical critical exponent involved in the slowing down of the decay rate $\Gamma_q^- \approx \omega_e / (\xi/a)^z f(q\xi)$, while $f(q\xi)$ is an homogeneous function of the form $f \approx [1 + (q\xi)^2]^{-1}$. The exponent η is expected around 0.2 for dimensionality of the system $d=3$. For a critical behavior $\xi \propto (T-T_N)^{-\nu}$ one has a divergence of T_1^{-1} of the form $T_1^{-1} \propto (T-T_N)^{-n}$, with the exponent n given by $n = \nu(z-1-\eta) = \gamma - \nu(3-z)$, γ being the critical exponent describing the divergence of the staggered susceptibility. The temperature dependence of the relaxation rate in the PM phase (Fig. 6) is consistent with a critical law with a small, little x -dependent exponent n . It has been shown by Spalek *et al.*¹⁷ that in the high-temperature approximation the behavior of the homogeneous susceptibility in a randomly dilute Heisenberg paramagnet is still of the Curie-Weiss form, with a renormalization of the Curie constant $C = C_0(1-x)$ and of the Curie-Weiss temperature $\theta_N = \theta_N^0(1-x)$. For simple cubic Ising systems with random impurities, Monte Carlo calculations¹⁸ do not indicate a sizeable change of the critical exponents and the temperature behavior of the susceptibility is virtually independent of concentration. Our estimates of n (Fig. 6) are consistent with the aforementioned predictions.

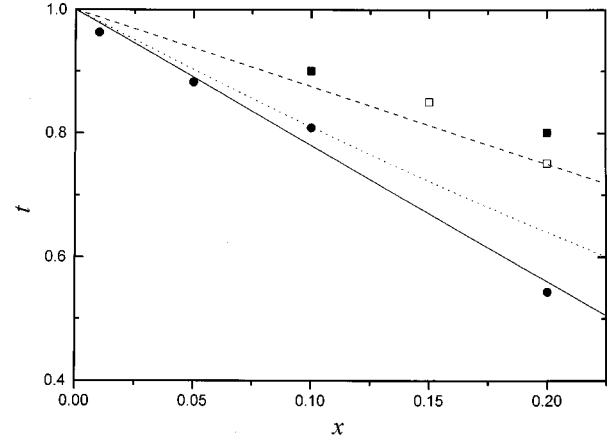


FIG. 7. Reduced Néel temperature $t = T_N(x)/T_N(0)$ as a function of the lithium content in $\text{Ni}_{1-x}\text{Li}_x\text{O}$ (●, present work) and comparison with the one in Mg-doped NiO (open square, solid square) (Refs. 19, 21, and 22). The solid line is the linear best-fit behavior, yielding $t = 1 - 2.2x$, while the dashed line is the theoretical line for simple cubic Heisenberg systems with a NN interaction only and the dotted line the form resulting from a crude dilution model (see text).

As regards the doping dependence of the Néel temperatures (Fig. 7) the behavior of $t = T_N(x)/T_N(0)$ for Li-doped NiO is compared with the one for Mg-doped NiO (Ref. 19) and with the theoretical predictions for the simple diluted Heisenberg models. Due to the hopping of the holes, the decrease of t with x is faster than the one induced by Mg. An analogous effect has been observed in La_2CuO_4 by Cheong *et al.*²⁰ On the other hand, the behavior of t with x is surprisingly close to the one predicted by a crude dilution model. In a mean-field approximation, the Néel temperature in NiO depends only on the next-NN exchange interaction J_2 , because of the cancellation of the field from the 12 NN for symmetry reasons and one has $T_N \propto J_2$. If in the Hamiltonian $J_2 \vec{S}_i \cdot \vec{S}_j$ one weights with $(1-x)$ the probability of having a magnetic ion at a given site, then $t \propto (1-x)^2$ (dotted line in Fig. 7). The agreement is probably fortuitous, also in view of the partial contradiction of the dilution model with more quantitative theoretical descriptions.¹⁷

The broadening δH of the ${}^7\text{Li}$ NMR line on approaching T_N can be analyzed in terms of the temperature dependence of the susceptibility, since $\delta H \propto \chi_a$ (Sec. II B). Theoretically, from the expression of the homogeneous static susceptibility in randomly diluted paramagnets,¹⁷ one would expect $\delta H \propto H_0 n(x) C(x) / [T - \theta_N(x)]$, namely, a moderate increase of δH on approaching T_N from above. The behavior of δH with T [Fig. 2(a)] is also consistent with the experimental observation for the susceptibility in Mg-doped NiO.¹⁹

On summarizing, the doping dependences of T_N and of the static susceptibility as well as of the spin lattice relaxation rate, on the whole, appear to indicate that a dilutionlike picture, with a renormalization of the Néel temperature and of the Curie-Weiss constant and small corrections of the critical exponents, can describe the main features deduced from NMR spectra and relaxation in the paramagnetic phase of Li-doped NiO.

B. High-temperature AF phase (AF I)

From the NMR spectra below $T_N(x)$ one can extract the temperature dependence of the field h_{AF} at the Li site result-

ing from the ordering of Ni^{2+} magnetic moments, as described in Sec. II. In Fig. 4 it is shown how a critical behavior yielding $h_{\text{AF}} \propto \langle \mu_{\text{Ni}} \rangle \propto (T_N - T)^{1/3}$ can qualitatively describe the temperature dependence of the sublattice magnetization for $T/T_N(x) \geq 0.7$. Also, for the sample at $x=0.2$, the results (not reported) are consistent with this critical law. The departure occurring below $T/T_N \approx 0.7$ cannot be accounted for by the crossover to a mean-field behavior and it is most likely related to the localization of the holes (next section).

As regards the ${}^7\text{Li}$ relaxation rates, it is noted that in a pure AF the temperature behavior would be quite different from the ones shown in Fig. 5. In a pure AF the spin excitations driving the nuclear relaxation process are magnons, corresponding to conventional underdamped spin waves. As in CuO ,¹⁰ Li doping alters the spin fluctuations in a dramatic way. The relaxation rate increases by orders of magnitude and displays marked maxima at a temperature T_m which is a function of x and of the measuring frequency ω_L . These features are due to a direct relaxation process, with a $\omega \rightarrow 0$ spectral density of the hyperfine field at the nucleus that, negligible in the pure AF, is enhanced by doping. The insurgence of low-energy spin excitations has to be related to a diffusionlike motion of the holes, with an effective correlation time of the form

$$\tau_h \approx \frac{\tau_0}{n_h} = \frac{\tau_0}{x} \exp[E_g(x)/T], \quad (8)$$

n_h being the fraction of itinerant holes and $E_g(x)$ the energy gap between localized and itinerant states.¹⁰ The direct relaxation process is induced when the passage of the hole close to the Li site causes a disturbance in the AF matrix (for instance, a magnetic polaron) which locally anneals the field resulting from the undisturbed magnetic moments.

The features of the ${}^7\text{Li}$ relaxation rate in the AF I region are consistent with the theoretical picture outlined above, the passage of the hole causing the $\text{Ni}^{2+} \leftrightarrow \text{Ni}^{3+}$ fluctuations.⁹ For the nuclear relaxation this corresponds to a fluctuating dipolar field at the Li site. Starting from Eq. (1) and considering the field $h(\vec{r}, t)$ associated with a hole at \vec{r} and corresponding to an effective magnetic moment $\epsilon \mu_B$, for a correlation function for the diffusion process of exponential character, the relaxation rate can be written

$$2W = \frac{\gamma^2}{6} (\epsilon \mu_B)^2 \int_v \frac{c_h}{r^6} (2 + \sin^2 \theta) \frac{2\tau_h}{1 + \omega_L^2 \tau_h^2} r^2 dr d\Omega, \quad (9)$$

where c_h is the hole concentration. By assuming for simplicity a single correlation time τ_h not depending on \vec{r} , Eq. (9) leads to

$$2W = \frac{8\pi}{9} \gamma^2 (\epsilon \mu_B)^2 \frac{c_h}{d_m^3} \frac{2\tau_h}{1 + \omega_L^2 \tau_h^2}, \quad (10)$$

where d_m is the distance of the minimum approach of the hole to Li^+ .

The experimental data in the AF I phases (see Fig. 5) have been fitted in the light of Eq. (10) and the values of the energy gaps $E_g(x)$ and of τ_0 have been extracted (Fig. 8).

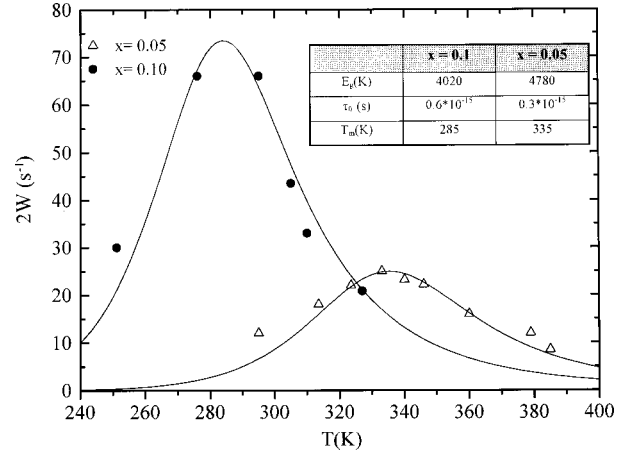


FIG. 8. Comparison of the experimental results for ${}^7\text{Li}$ relaxation rates in $\text{Ni}_{1-x}\text{Li}_x\text{O}$ with the theoretical prediction (solid lines) according to the model of low-energy spin excitations driven by hole diffusion. In the inset the best-fit values are reported.

E_g can be compared with the one estimated for the hopping of polarons from resistivity:⁶ $E_h \approx 3000$ K for $x \approx 0.02$. The decrease of E_g on increasing x , indicated by the resistivity and by ${}^7\text{Li}$ T_1 's, is strong support for the hypothesis of gaps between itinerant and localized states of cooperative character, reduced by charge doping, similarly to the case of lanthanum oxides.¹⁶ E_g for NiO is significantly larger than in CuO [where $E_g(x=0.03) \approx 200$ K], in qualitative agreement with the increase of the binding potential. Furthermore, E_g is remarkably close to the effective exchange interaction between Ni^{2+} and the O-2p hole estimated by Kuiper *et al.*⁴ Also the dielectric data²³ for the high-temperature absorption peaks in the loss tangent can consistently be interpreted in terms of a hopping process of the polarons. From our estimates of τ_0 and E_g for $x=0.1$ one expects that in the measurements at 100 kHz the peak in the loss tangent occurs around 210 K, consistent with the observation at about 190 K for $x=0.07$.²³ Finally, it is noted that from the value of $2W$ at T_m , where according to Eq. (10) one has $\tau_h = \omega_L^{-1}$, one derives for the factor ϵ the value $\epsilon \approx 5 \times 10^{-2}$, if d_m is assumed to coincide with the Ni-Ni distance.

C. AF phase II

Below T_m , the hopping frequencies of the holes become very small ($\tau_h \omega_L \gg 1$). Measurements at different fields $H_0 = \omega_L / \gamma$ indicate the occurrence of the slow-motion conditions [see Eq. (10)] and one can consider T_m as a freezing temperature for charge fluctuations. Below T_m the holes are localized and changeovers in the relaxation mechanism, in the recovery laws, and in the temperature dependence of the AF field can be expected. These effects have been evidenced in CuO (Ref. 11) as well as in Sr-doped La_2CuO_4 .²⁴

A variety of experimental findings indicates that in $\text{Ni}_{1-x}\text{Li}_x\text{O}$ the charge compensating holes are primarily on the oxygen around the Li impurity.²⁵ The antiferromagnetic coupling of the oxygen hole with the Ni spin results in a magnetic moment, a kind of spin texture onto the AF matrix. Dielectric loss measurements show that the Li^+ centers have associated electric dipole moments.²⁵

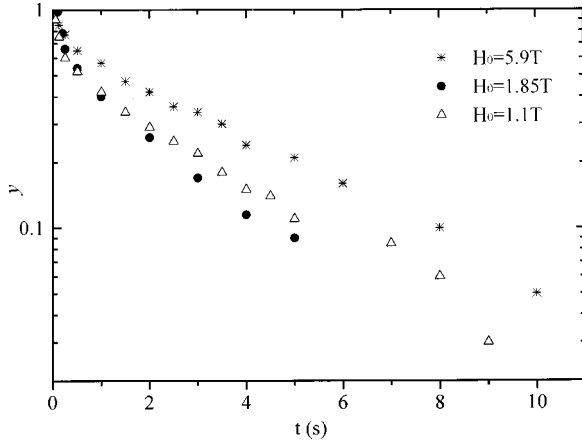


FIG. 9. ${}^7\text{Li}$ spin lattice relaxation recoveries in $\text{Ni}_{0.9}\text{Li}_{0.1}\text{O}$ at $T \approx 20$ K as a function of the strength of the field. The recoveries of the echo amplitude $y = [s(\infty) - s(t)]/s(\infty)$ as a function of the time t after the saturation, in zero-field-cooled and in field-cooled conditions, in $H_0 = 1.1$ T, are the same within the experimental errors.

The dramatic increase, on cooling, of the ${}^7\text{Li}$ relaxation rate (see Fig. 5) is the most direct evidence that spin fluctuations still occur after charge freezing. This observation is analogous to the one²⁶ in the AF phase of Zn-doped La_2CuO_4 , where the spin vacancy due to the $S=0$ Zn^{2+} for Cu^{2+} $S=1/2$ substitution induces the anomalous magnetic moment. We point out that the marked peaks in the relaxation rate have been corroborated by muon spin relaxation (μSR).²⁷ In $\text{Ni}_{0.95}\text{Li}_{0.05}\text{O}$, the depolarization rate, in the internal field at the muon site, on cooling increases by a factor of about 10^4 , with a maximum at $T \approx 130$ K. Besides confirming our findings, this observation rules out the hypothesis that reorientations of the electric dipoles around Li can be responsible for the enhancement of the relaxation rate, through the interaction of the electric field gradients with the ${}^7\text{Li}$ quadrupole moment.

The temperature $T^* \approx 130$ K where the relaxation rates have their maxima and the activation energies (see later on) do not depend on the doping amount, at least for small x . This is further support in favor of a relaxation mechanism involving the fluctuations of a local effective magnetic moment $\vec{\mu}_e$ around the Li impurity. The random spatial distribution of the $\vec{\mu}_e$'s and the character of their long-range interaction via the AF matrix are features common to spin glass systems. The freezing of the spin fluctuations can be heuristically described by a correlation function for $\vec{\mu}_e(t)$ of exponential character, with a distribution of correlation time $p(\tau_\mu)$ accounting for the spin-lattice recovery in the form of a stretched exponential (Fig. 9). Then the ${}^7\text{Li}$ relaxation rate can be written

$$2W = \frac{\gamma^2}{2} h_{\text{eff}}^2 \int p(\tau_\mu) \frac{2\tau_\mu}{1 + \omega_L^2 \tau_\mu^2} d\tau_\mu, \quad (11)$$

where h_{eff} is an effective amplitude of the fluctuating field. A possible form of distribution of τ_μ is the one corresponding to a rectangular distribution in the activation energies, thus yielding τ_μ ranging from $\langle \tau_\mu \rangle / b$ to $\langle \tau_\mu \rangle b$, with $\langle \tau_\mu \rangle \propto \exp[\langle E_A \rangle / T]$. Then²⁸

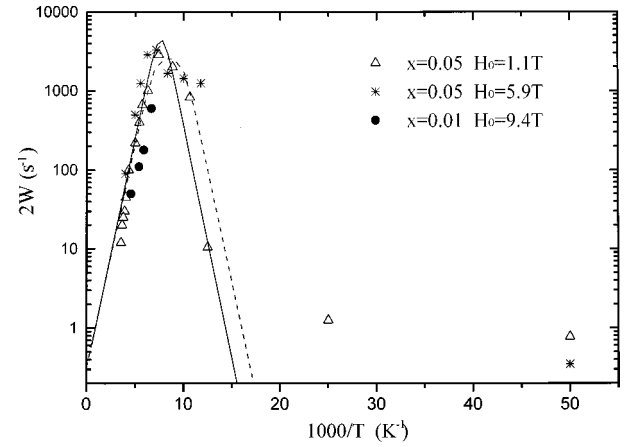


FIG. 10. Semilogarithmic plot of the ${}^7\text{Li}$ relaxation rates in the AF II phase vs T^{-1} in the samples at $x=0.01$ and $x=0.05$, for different external fields. The lines represent the theoretical behaviors predicted by Eq. (10) for $b=1$ (monodispersive relaxation process, solid line) and $b=10$ (dashed line).

$$2W = \frac{\gamma^2}{2} h_{\text{eff}}^2 \frac{1}{\omega_L \ln b} [\tan^{-1}(\omega_L \langle \tau_\mu \rangle b) - \tan^{-1}(\omega_L \langle \tau_\mu \rangle / b)]. \quad (12)$$

In Fig. 10 the relaxation rates in the AF II phase are compared with this theoretical behavior. For a moderate width of the distribution ($b \leq 10$) the temperature behavior is not much different from the one for a simple Arrhenius-type law for $\langle \tau_\mu \rangle$, particularly in the temperature region of fast fluctuations, namely, $\tau_\mu \omega_L \leq 1$. The average activation energy is approximately $\langle E_A \rangle \approx 1300$ K and seems practically independent of the amount of lithium, at least for small x . Also the effective field $h_{\text{eff}} \approx 80$ G, as derived from the maximum in the relaxation rate [where $\langle \tau_\mu \rangle \approx 1/\omega_L$, see Eq. (11)], is approximately independent of x . The value of the effective field corresponds to a magnetic moment of about $0.25\mu_B$ at the O site, for $H_0 = 1.1$ T.

The magnetic field appears to affect the properties of the system of the magnetic moments superimposed on the AF matrix. In fact, on varying the external field H_0 one should observe the ω_L dependence predicted by Eq. (10), which in the regime of extreme slowing down, namely, $\omega_L |\tau_\mu| \gg 1$, predicts $T_1^{-1} \propto \omega_L^{-\alpha}$, with $1 \leq \alpha \leq 2$ depending on the width of the distribution. This dependence is not observed. The discrepancy could be due to a field-dependent phase diagram, a rather common situation in disordered magnets with competing interactions and/or spin anisotropies.²⁹ On the contrary, the lack of a field dependence indicative of the slow motion condition for $T < T^*$ and the fact that T^* is little, if any, x dependent are in favor of a real phase transition to an ordered state. On the other hand no modification in the linewidth has been detected at T^* and also the stretched exponential recovery is a condition typical of a spin glass state rather than of a phase transition. Further work is in progress through susceptibility and μSR measurements to clarify this interesting point.²⁷

IV. SUMMARIZING REMARKS AND CONCLUSIONS

By means of a thorough analysis of ${}^7\text{Li}$ NMR spectra and spin-lattice relaxation in $\text{Ni}_{1-x}\text{Li}_x\text{O}$, the effects of charge

doping in antiferromagnetic $S=1$ NiO have been studied. In the paramagnetic phase the spin vacancies at the lattice positions where $\text{Li}^+ S=0$ substitutes $\text{Ni}^{2+} S=1$ break the symmetry of the AF correlated spin fluctuations. Thus the enhancement and slowing down of the fluctuations cause a time-dependent field at the Li site, yielding a divergence in the relaxation rate when the Néel temperature is approached from above. This divergence turns out to be described by a small (≈ 0.2) critical exponent, little x dependent and in general agreement with the main aspects of a randomly diluted Heisenberg paramagnet. From the relaxation rates and from the broadening of the NMR spectra, the doping dependence of the Néel temperature has been derived, up to the doping amount $x \approx 0.20$ where the cubic AF structure of NiO is still preserved. For $x \leq 0.1$ one has $T_N(x) \approx T_N(0)[1 - 2.2x]$. The reduction of T_N with doping appears faster than for homovalent substitutions as in other charge-doped AF's, the hopping of the holes being strongly effective in destroying the long-range order.

In the AF phase the hole itinerancy involves the spin dynamics of the ordered Ni^{2+} magnetic moments and induces a shift of the spectral distribution of the magnetic excitations towards low energies. Then the ${}^7\text{Li}$ relaxation rates, instead of being driven by magnons scattering as in pure AF's, are controlled by the fluctuations in the hyperfine field when the passage of the hole locally forms a singlet and anneals the order in the Ni^{2+} magnetic moments. A correlation time of the form $\tau_h \propto \exp[E_g(x)/T]$ can be introduced, E_g being the gap from localized to itinerant states. Thus in the AF I phase the relaxation rate exhibits maxima at $T = T_m$, when τ_h^{-1} reaches the radio-frequency range. The strength of these maxima is x dependent, as well as the temperature T_m . The gaps $E_g(x)$ have been estimated and turn out to be larger than in other TMO's and decreasing when the doping is increased, in general agreement with electrical conductivity. The NMR line broadening below T_N is due to the sublattice magnetization $\langle \mu_{\text{Ni}} \rangle$ and information on its temperature dependence has been obtained. While close to $T_N(x)$ the growth of $\langle \mu_{\text{Ni}} \rangle$ is approximately described by the usual critical law, for $T/T_N(x) \leq 0.7$ one notes a departure and this

has been considered a signature of localization of the holes. In the temperature region below the localization, a new source of spin excitations has been evidenced. The ${}^7\text{Li}$ relaxation rates increase by three orders of magnitude on cooling, with marked maxima at a temperature T^* . The strength of the maxima, as well as T^* , does not depend on the amount of doping, at least for small x , supporting a picture of a local relaxation mechanism. The stretched exponential form of the recovery law suggests a distribution of correlation times τ_μ for the fluctuations of the extra magnetic moments $\vec{\mu}_e$. Measurements of muon depolarization rates confirm an extreme slowing down of the spin fluctuations and also rule out any possible role of the electric dipoles around the Li^+ impurities in driving the relaxation process through the time-dependent quadrupolar interaction. From the fitting of the temperature dependence of ${}^7\text{Li}$ relaxation rates the average activation energy for the reorientation of the μ_e 's turns out $\langle E_A \rangle \approx 1300$ K, again practically independent of x . The amplitude of the fluctuating field is around 80 G, corresponding to an effective magnetic moment of about $0.25\mu_B$ at the Li-O distance. Below T^* the relaxation rate decreases by several orders of magnitude on cooling. In principle this could be related either to a phase transition to an ordered state with a real nonzero local order parameter or to an extreme slowing down of the magnetic moments. Measurements at different magnetic fields do not clarify this point. The relaxation rates below T^* are almost field independent, as expected for a real phase transition to an ordered state. However, no modification of the width of the broad NMR spectra is detected below T^* , consistent with $\langle \mu_e \rangle \neq 0$ and then with a spin glass state. In this case our findings indicate that the external field affects the properties of this spin glass state.

ACKNOWLEDGMENTS

S. Aldrovandi is gratefully acknowledged for his technical assistance in many aspects of the experiments. P. Carretta is thanked for useful discussions and for having provided the results of the muon measurements before publication. The research has been carried out with financial support from INFN (Grant No. VORS) and from INFM.

*Present address: Department of Solid State and Applied Physics, Material Science Center, Nijenborgh 4, 9747 Groningen, The Netherlands.

¹N. F. Mott, *Metal-Insulator Transitions* (Taylor & Francis, London, 1990).

²See G. A. Sawatzky, in *Early and Recent Aspects of Superconductivity*, edited by J. G. Bednorz and K. A. Müller (Springer-Verlag, Berlin, 1990), p. 345 and references therein.

³G. Srinivasan and M. S. Seehra, *Phys. Rev. B* **29**, 6295 (1984).

⁴P. Kuiper *et al.*, *Phys. Rev. Lett.* **62**, 221 (1989).

⁵G.F. Dionne, *J. Appl. Phys.* **67**, 4561 (1990), and references therein.

⁶R. R. Heikes and W. D. Johnston, *J. Chem. Phys.* **26**, 582 (1957).

⁷J. E. Keem, J. M. Honig, and L. L. Van Zandt, *Philos. Mag. B* **37**, 537 (1978).

⁸F. Zhang and T. M. Rice, *Phys. Rev. B* **37**, 3759 (1988).

⁹E. Dagotto, J. Riera, A. Sandvik and A. Moreo, *Phys. Rev. Lett.* **76**, 1731 (1996).

¹⁰P. Carretta, M. Corti, and A. Rigamonti, *Phys. Rev. B* **48**, 3433 (1993).

¹¹P. Carretta, F. Cintolesi, and A. Rigamonti, *Phys. Rev. B* **49**, 7044 (1994).

¹²V. Massarotti, D. Capsoni, and M. Bini, *Z. Naturforsch. Teil A* **50**, 155 (1994).

¹³W. Li, J. N. Reimers, and J. R. Dahn, *Phys. Rev. B* **46**, 3236 (1992).

¹⁴K. Hirokawa *et al.*, *J. Phys. Soc. Jpn.* **54**, 3526 (1985).

¹⁵F. Borsa and A. Rigamonti, in *Magnetic Resonance at Phase Transitions*, edited by F. J. Owens, C. P. Poole, and H. A. Farach (Academic Press, New York, 1979), p. 109; H. Benner and J. P. Boucher, in *Magnetic Properties of Layered Transition Metal Compounds*, edited by L. J. de Jongh (Kluwer, Dordrecht, 1990), p. 323.

¹⁶For details in the derivation, besides Ref. 15, see A. Rigamonti *et al.*, in *Early and Recent Aspects of Superconductivity*, edited by J. G. Bednorz and K. A. Müller (Springer-Verlag, Berlin,

- 1990), p. 441; P. Carretta, A. Rigamonti, and R. Sala, *Phys. Rev. B* **55**, 3734 (1997).
- ¹⁷J. Spalek *et al.*, *Phys. Rev. B* **33**, 3407 (1986).
- ¹⁸D. P. Landau, *Phys. Rev. B* **22**, 2450 (1980).
- ¹⁹Zheng Feng and M. S. Seehra, *Phys. Rev.* **45**, 2184 (1992).
- ²⁰S-W. Cheong, A. S. Cooper, L. W. Rupp, B. Battlog, J. D. Thompson, and Z. Fisk, *Phys. Rev. B* **44**, 9739 (1991); see also Ref. 26.
- ²¹A. Arkhipov, *Fiz. Tech. Zinatnu Serija* **3**, 24 (1981).
- ²²R. B. Stinchombe, *J. Phys. E* **12**, 4533 (1979).
- ²³E. Iguchi and K. Asaki *J. Phys. Soc. Jpn.* **61**, 3385 (1992).
- ²⁴F. Borsa *et al.*, *Phys. Rev. B* **57**, 7334 (1995).
- ²⁵See J. van Elp, H. Eskes, P. Kuiper, and A. Sawatzky, *Phys. Rev. B* **45**, 1612 (1992), and references therein.
- ²⁶M. Corti, A. Rigamonti, F. Tabak, P. Carretta, F. Licci, and L. Raffo, *Phys. Rev. B* **52**, 4226 (1995).
- ²⁷P. Carretta, A. Lascialfari, and F. Tedoldi (unpublished).
- ²⁸A. Rigamonti and S. Torre, *Phys. Rev. B* **33**, 2024 (1986).
- ²⁹L. J. De Jongh, in *Magnetic Phase Transition*, edited by M. Ausloos and R. J. Elliot (Springer-Verlag, Berlin, 1983), p. 172.